Dynamical screening of the exciton resonance in conjugated polymers/carbon nanotubes composites

Larry Lüer,[1,2,*] Sajjad Hoseinkhani,[1] Moreno Meneghetti,[3] and Guglielmo Lanzani[4]
[1]*CNR/INFM, Politecnico di Milano, Milano, Italy*
[2]*Madrid Institute for Advanced Studies, IMDEA Nanociencia, Madrid, Spain*
[3]*Dipartimento di Scienze Chimiche, Nanophotonic Laboratory, Università di Padova, Padova, Italy*
[4]*Center for Nano Science and Technology, IIT@POLIMI, Milano, Italy*
(Received 14 September 2009; revised manuscript received 19 January 2010; published 5 April 2010)

We study coherent phonons in polymer-carbon nanotubes composites by sub-10-fs pump-probe spectroscopy. We find that coherent phonons in the polymer network modulate the exciton resonance of the wrapped nanotube. We propose a model of dynamic environmental coupling in which the polymer vibration affects the carbon nanotubes exciton energy by virtue of the modulation of its dielectric screening. Carbon nanotubes act as antenna for the local environment and highlight small changes in the dielectric constant. This shows the extreme sensitivity of carbon nanotubes to their surrounding, a property essential for sensing applications and crucial for understanding composite materials.

DOI: 10.1103/PhysRevB.81.155411 PACS number(s): 78.47.J−, 73.22.−f

Carbon nanotubes (CNTs) are thin, hollow cylinders of carbon atoms in sp^2 hybridization with π electrons distributed over their surface.[1] This leads to the quasi-one-dimensional electronic properties and also to their high sensitivity to the surrounding. In particular, the sharp resonances of the one-dimensional excitons are strongly affected by the dielectric properties of the medium which modify Coulomb screening and consequently the self energy, the binding energy[2] and the Sommerfeld factor.[3] CNTs come in a variety of forms and properties. In order to improve handling and separation, chemical functionalization has been pursued rather extensively.[4,5] This has advantages, such as the control and the huge potential of the organic chemistry, but also drawbacks. Chemical functionalization introduces defects, is a complicated process and may lead to undesired selectivity in diameters. Alternatively a much simpler approach is that of the noncovalent "functionalization." Here aromatic interactions lead to complex architectures where the conjugated system wraps around the tube.[6,7] The interaction is driven by chemical or topological affinity and turns out to be selective in chirality. The physics of such hybrid heterojunctions brings about the concept of the *van der Waals interface*.[8] Besides charge and energy transfer[9] between the conjugated polymer and the CNT, anomalous charge transport and carrier thermalization, quenching of the emission, and resonance smearing are attributed to such interfaces.

It is common sense that near future applications of CNT are in networks or composite materials. As a practical advantage, composites do not require fancy nanoprobes for testing or exploitation and their preparation is suitable for large scale industrial production. A proper engineering of these composites requires however a deep understanding of the environmental influence on CNT properties which is at present still missing.

Here we report a study on CoMoCat CNT wrapped into two kinds of conjugated polymers with largely different optical gap and phonon energy, namely, poly(9,9-dioctylfluorenyl-2,7-diyl) ("PFO," optical gap approximately 3.0 eV and main C=C stretching frequency of 1600 cm^{-1}) and regioregular poly-(3-hexylthiophene-2,5 diyl) ("P3HT," optical gap approximately 1.9 eV and C=C stretching frequency about 1450 cm^{-1}). Such conjugated polymers form an ordered arrangement around some tubes of proper chirality, according to patterns not fully known yet. We use steady state and transient absorption spectroscopy for investigating our samples and detect coherent phonon spectra which bring a wealth of information about the vibronic dynamics.[10–13] We find that the effect of polymer wrapping can be clearly seen in the optical resonances. In particular, the nanotubes influence the polymer network morphology while the polymer affects the excitonic resonances of the nanotubes. Dielectric screening however is not just a static effect but can be modulated at terahertz frequency by coherent phonons which represents collective, in-phase vibration of the carbon atoms in the polymer chains.

Samples of PFO:CNT and P3HT:CNT have been prepared according to a procedure adopted by Chen *et al.*[14] for the preparation of the PFO adduct. Briefly, PFO (purchased from American Dye Source) or P3HT (purchased from Sigma-Aldrich) and CoMoCat were dispersed in toluene in the first case and in chloroform in the second case by ultrasonication. Then a centrifugation at 10 000*g* allowed to separate strongly bundled nanotubes. The supernatant was separated and used to obtain thin films on cover slips by air spraying the solutions.

We perform pump-probe spectroscopy with 7 fs broadband pulses that span the wavelength region from 500 to 700 nm in a single-shot detection scheme, allowing us to obtain probe wavelength profiles of vibrational amplitudes and phases in the frequency range of 20–2200 cm^{-1}. Details about our setup and the working principle of our technique can be found in Ref. 15.

Figure 1 shows the ground-state absorption spectra of PFO:CNT and P3HT:CNT, compared to the spectra of the respective pure polymer films (panels a and b, respectively). The presence of the carbon nanotubes is evidenced by a series of sharp excitonic transitions E_{11} around 1.2 eV. In PFO:CNT, the E_{22} region around 2.1 eV can be observed as

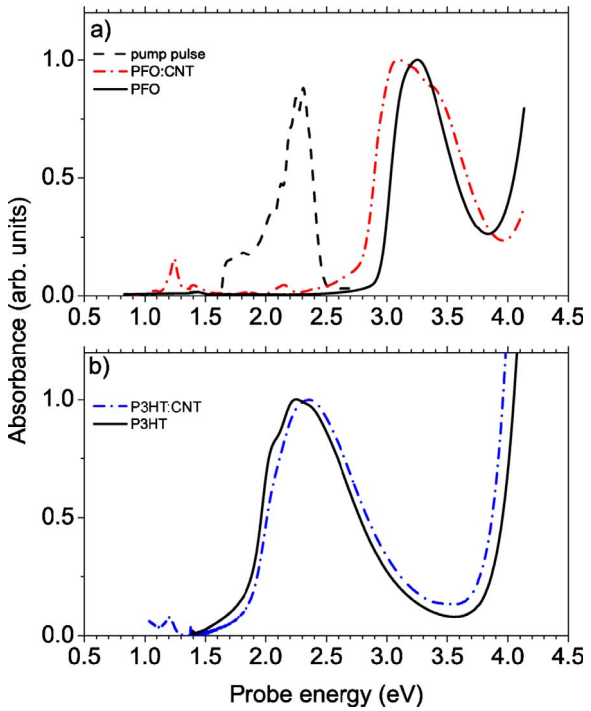

FIG. 1. (Color online) Ground-state absorption spectra of PFO:CNT and P3HT:CNT samples compared to the pure polymer spectra (panels a and b, respectively). In Fig. 1(a), the scattering contribution introduced by the nanotubes has been subtracted by a polynomial. The pump spectrum is given as dashed line.

well while in P3HT:CNT, it is superposed with the strong optical transition of polythiophene. Comparing the total oscillator strengths of the nanotubes and the polymer gives an order of magnitude estimate for their relative abundances, important for subsequent modeling. In polymers, the cross section per sp^2 carbon atom[16] is on the order of $\sigma_{C,Polymer} \approx 10^{-17}$ cm^2, similar to the one of (6,5) carbon nanotubes.[17] Considering the uncertainty in this evaluation we estimate that sp^2 carbon atoms in CNT account for a minimum of 5% to a maximum of 20% of the total amount. A complete "monolayer" of polymer wrapped around a CNT should have a C(sp^2) atom ratio of $C_{polymer}/C_{CNT} < 1$ due to the presence of hydrogens and aliphatic (nonconjugated) side groups. Therefore, we conclude that there is a large fraction of the polymer segments that are *not* in direct contact with the CNT. This causes a heterogeneous morphology in the polymer phase; consequently, in the photophysical description, polymer-polymer interactions (bulklike behavior) will be as important as polymer-CNT interactions.

The embedded CNTs induce small, yet detectable changes in the absorption spectrum of the polymer. The pristine PFO is characterized by a structureless absorption band with an absorption edge at 3.0 eV. In the PFO:CNT sample, the optical band gap is reduced by 0.2 eV and a vibronic structure appears in the line shape. We assign these changes to the planarization of the polymer chain near the tube. The driving force is probably the aromatic π-π interaction between the fluorene units in the PFO and the graphenelike CNT surface which favors the face to face adjustment and causes a reduction in the inter-ring torsional angles. The effect will replicate itself also in the second PFO shell, leading overall to a significant redshift of the optical spectra. We highlight that in the case of PFO:CNT, there is no sharp onset of absorption as in the case of pure PFO; instead, a tailing is observed that extends well into the range of the broadband pulses that we use for transient spectroscopy [given as dashed lines in Fig. 1(a)]. It follows that even though a large fraction of the PFO segments is not in close contact with CNT, we will selectively excite only those segments that are structurally modified due to the vicinity of CNT.

The absorption spectrum of pure regioregular P3HT films is a superposition of the contribution of highly ordered regions, two-dimensional stacked lamellae with vibronic maxima at 2.09 and 2.18 eV, and of amorphous regions peaking at 2.39 eV and without vibronic structure.[18] Here the introduction of CNT has the opposite effect compared to PFO:CNT: it leads to a *loss of ordering*, as suggested by the reduced vibronic structure and the blueshift. A multipeak analysis shows that this blueshift is not caused by the electronic gap change but rather by the higher weight of the amorphous against the ordered contribution.

In summary, in spite of their relatively small fraction in weight, CNTs affect the surrounding polymer environment: the amorphous PFO undergoes a planarization of the chain conformation upon wrapping around the tube; the highly ordered P3HT is "disturbed" by the tube, and loses some interchain correlation.

In Fig. 2 we present a zoom of the absorption spectra into the region of the E_{11} transition for pure CoMoCat,[19] PFO:CNT, and P3HT:CNT samples (panels a–c, respectively). A series of excitonic resonances are observed in the region from 0.8 to 1.5 eV. By fitting of the most prominent features we obtain nine Voigt bands, which can be assigned to respective chiralities via comparison with previously characterized samples. The fit also includes the first vibronic replica of the CNT absorption. For the pure CoMoCat sample, we obtain a good fit if we apply a global energy shift of $\Delta E_{gl} = -22.5$ meV to all nine chiralities. This global shift reflects the difference in the "stationary" environmental dielectric constant between our sample in sodium cholate and the reference sample, in sodium dodecyl sulfate.[20] For the "wrapped" samples PFO:CNT and P3HT:CNT, we obtained a good fit if we applied a global shift of −12 meV and −43 meV, respectively, to all nine chiralites and an additional *specific* redshift to two of the 9 chiralities (for details, see caption of Fig. 2).

In the case of the "wrapped" samples in Figs. 2(b) and 2(c), the *global* shift can be either due to a change in the stationary dielectric constant of the polymer phase (and its concomitant effect on the exciton resonance) or due to mechanical strain exerted by the polymer. Among the three samples under study, the P3HT has the highest dielectric constant due to the high polarizability of the sulfur atoms. Since the highest *global* shift occurs for P3HT:CNT, this suggests that the effect is dominated by a change in the dielectric constant. Mechanical strain, on the other hand, is exerted when binding motifs and/or sterical requirements force the polymer:CNT system into a minimum-energy geometry in which the CNT has reduced radial/translational symmetry. Mechanical strain—and in consequence its effect

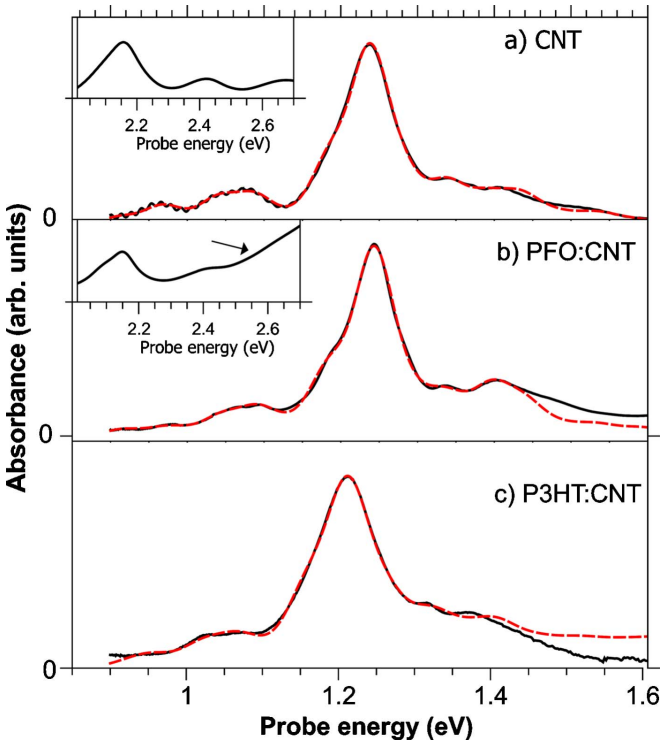

FIG. 2. (Color online) Ground-state absorption spectra of pure CNT, PFO:CNT, and P3HT:CNT samples (panels a–c, respectively). Black (full curves): experimental curves; red (dotted curves): fitted curves using a multi-Voigt band approach with the following parameters; Gaussian width: 0.04 eV except for panel c (0.045 eV), Lorentzian width 0.02 eV, intensity ratio $I(E_{11}+G)/I(E_{11})=0.14$. The E_{11} energies are taken from Ref. 20. In order to fit our different environments, global energy shifts have been introduced: (a) −22.5 meV, (b) −12 meV, and (c) −43 meV. In the wrapped samples [(b) and (c)], some chiralities were additionally shifted to fit the data: panel b, −8 meV for both (7,5) and (9,1) tubes and panel c, −8 meV for (6,5) tube and −10 meV for (7,5) tube. The insets of panels (a) and (b) show a zoom into the E_{22} region of the respective absorption spectra, after proper subtraction of the scattering background. The onset of the absorption of the CNT:PFO CT state is marked by an arrow.

on the excitonic resonances—should therefore depend on chirality and diameter of the CNT, as well as on the polymer under consideration. Moreover, the symmetry reduction on the CNT would lead to a broadening of the excitonic resonances, which we do not observe. In summary, we conclude that the global shift derives predominantly from a change in the dielectric constant while the effect of mechanical strain appears of secondary importance with respect to the CNT excitonic resonance. Note that which dielectric function has to be used, if ε_0 or ε_∞, depends on the exciton properties, particularly on its extension in space. The *e-h* correlation distance has been estimated to be around 2 nm (Ref. 21) and this, together with the one-dimensional character, is enough for justifying the use of the stationary dielectric function.

The specific—chirality and diameter dependent—energetic shift has been described in Ref. 9 for the cases of PFO and P3HT. The authors explained the effect by a matching between the "width" (lateral extension perpendicular to long molecular axis) of the polymer and the perimeter of the CNT, allowing complete coverage of the latter and thus maximum stabilization energy. They observed a specific stabilization[22] of the (7,5) tube, which is the one showing an additional redshift also in our case. This can be explained by the close contact of many strongly polarizable sulfur atoms on CNT with "matching" perimeter.

In the insets of Figs. 2(a) and 2(b), we show a zoom into the E_{22} region of the CNT absorption. In both cases, the absorption spectrum is dominated by the E_{22} resonance of the (6,5) tube at 2.15 eV. The onset of PFO absorption in the PFO:CNT sample becomes visible for energies around 2.5 eV. This shows that in this sample, the wrapped PFO can be resonantly excited with our broadband pulses that extend from 1.7 to 2.5 eV.

In the following we show transient absorbance spectra and the coherent phonon analysis. The later is achieved after subtraction of the "slow" time-dependent contribution in order to single out the high-frequency oscillating component. For each modulation frequency (Raman mode), we extract the amplitude of such modulation at each probe energy (coherent phonon spectra) and its phase. Such data are well understood in the molecular picture for the coherent phonon[23–25] and resemble the first derivative of Raman excitation profiles. There is a minimum in the amplitude at the 0-0 electronic transition and a corresponding sharp π flip in the phase spectrum, which describes the wave-packet traveling across the minimum of the potential-energy surface. Amplitude minimum and phase flip are then characteristic fingerprints of the vibronic transition modulated by the coherent state.

In Figs. 3(a) and 3(b), we show time-resolved absorption spectra of P3HT and P3HT:CNT, respectively, after pumping with 7 fs broadband pulses. In both cases, the pump-probe spectra show a transient bleach extending from 2.0 to 2.5 eV and a photoinduced absorption (PA) below 2.0 eV. The bleach spectrum is similar to the ground-state absorption spectrum, but with a different amorphous to crystalline ratio, due to the pump pulse resonance condition favoring the later. The PA band at 1.8–1.9 eV can be assigned to charged states in P3HT.[26] When normalized to same bleach, PA is clearly larger in P3HT:CNT than in P3HT, see Fig. 3(c). This may be due to a change in interchain interactions or to direct polymer-CNT charge transfer. We note that in the later case CNT spectral features (exciton bleaching) should appear but are not detected, being probably too weak and overwhelmed by the much stronger polymer contribution.

Fourier-transform (FT) spectra of pump-probe time traces are shown in Figs. 4(a) and 4(b) (for P3HT:CNT and P3HT, respectively). Both samples show a dominant band at 1440 cm^{-1}, which is assigned to the symmetrical C=C stretch vibration in the thiophene rings.[27] A weaker band, at 1370 cm^{-1} is also assigned to P3HT. According to this observation, coherent phonons are preferentially excited in P3HT.

Figures 4(c) and 4(d) show the FT amplitude and phase profiles as a function of probe energy for P3HT and P3HT:CNT, respectively, and for the main oscillation frequency at 1440 cm^{-1}. In pristine P3HT there is a clear am-

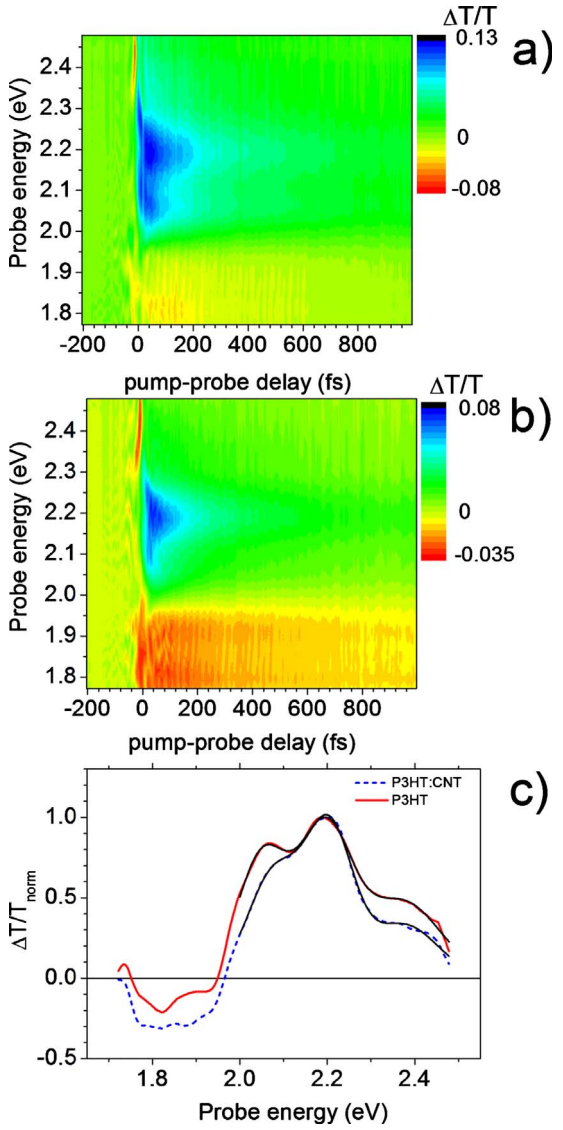

FIG. 3. (Color online) Time-resolved pump-probe spectra in (a) P3HT and (b) P3HT:CNT after pumping with 7 fs broadband pulses extending from 1.7–2.5 eV. (c) Single pump-probe spectra at 50 fs pump-probe delay for P3HT and P3HT:CNT (red and black curves, respectively). Thin black lines are multi-Gaussian fits to the data.

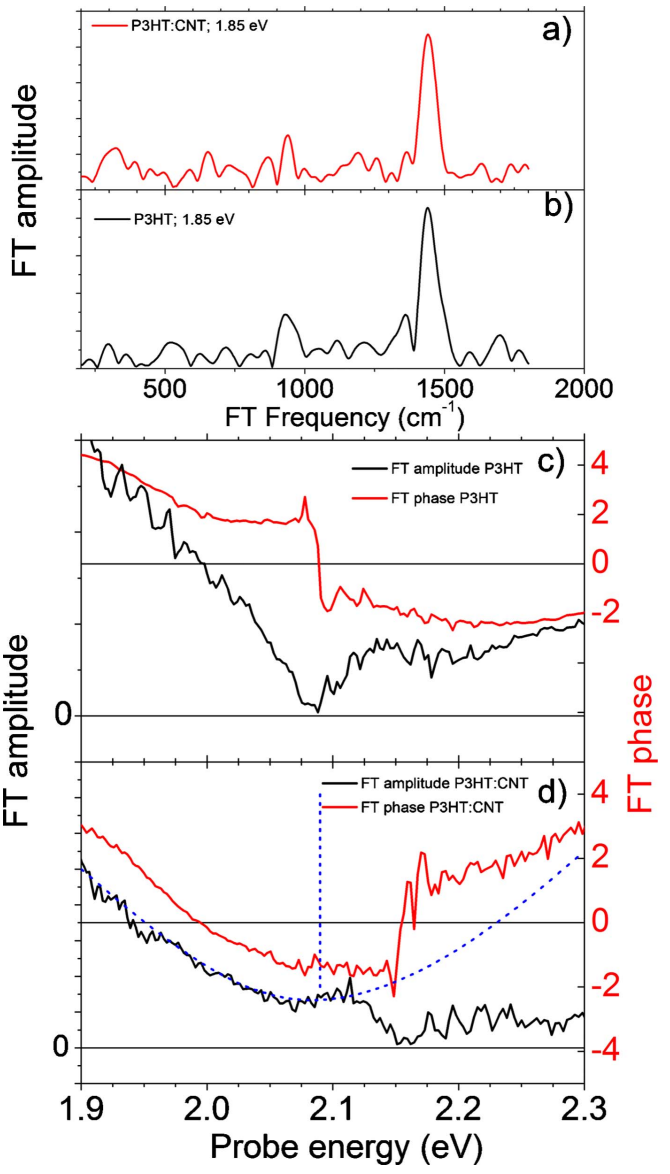

FIG. 4. (Color online) (a) Fourier-transform spectra of time traces at 1.85 eV for P3HT:CNT, after subtraction of population contribution using a global fit. (b) Same as (a) for pure P3HT. (c) FT amplitude (black) and phase (red) as a function of probing energy for P3HT. (d) Same as (c) for P3HT:CNT. Dashed blue lines are guides to the eye to evidence where the amplitude minimum of the P3HT phase in P3HT:CNT is expected.

plitude minimum and sharp π phase jump at 2.09 eV. By inspection of the absorption spectrum one sees that this energy corresponds to the maximum of the (00) transition of the ordered region, which is the one where coherent phonons are generated. The amplitude and phase profile in the P3HT:CNT sample is different [Fig. 4(d)]. Here the amplitude minimum and the phase jump occur at 2.16 eV, however there is no corresponding feature in the P3HT absorption spectrum. Surprisingly, 2.16 eV is precisely the maximum of the second excitonic resonance, E_{22}, in the (6,5) carbon nanotubes. We find the puzzling phenomenon that *the phonon of P3HT apparently modulates the exciton resonance of the (most abundant) CNT*. We propose that coherent phonons in the polymer matrix modulate the medium and that the CNT optical resonances, mediated by their environmental sensitivity, oscillate accordingly. Analogously to the analysis of the environmental effect on the cw absorption spectra (see Fig. 2), the effect on both the exciton binding energy and the self-energy contributes to the modulation of the exciton resonance energy. Note that due to the narrow linewidth of the CNT excitonic resonance, even a minor modulation of the resonance energy translates into a large coherent oscillation. It is important to add that in the wrapped sample P3HT:CNT, disorder reduces the vibronic structure compared to pure P3HT by increasing the linewidth and smears out the 00 resonance at 2.09 eV. The effect can be observed in absorption as well as transient absorption spectra, see Figs. 1(b) and 3(c), respectively. This reduces the visibility of coherent phonons. In consequence, only a broad minimum can be ob-

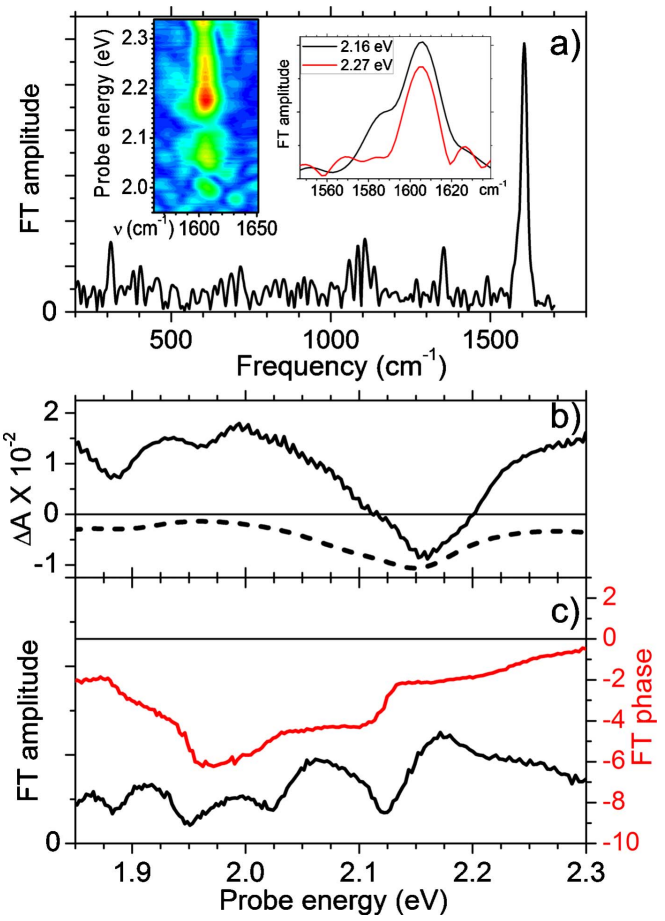

FIG. 5. (Color online) (a) FT spectrum at a probe energy of 2.16 eV. Left inset: FT map in the G mode and PFO CC stretch region. Right inset: horizontal cuts through left inset at two specific probe energies. (b) Pump-probe spectrum of PFO:CNT at $t=500$ fs after broadband pumping with 7 fs broadband pulses extending from 1.7 to 2.5 eV. The dashed line is minus the ground-state absorption spectrum. (c) Amplitude (black, lower curve) and phase (red, upper curve) profile at 1605 cm^{-1}. Please note that under our experimental conditions, the pure PFO sample is not excited and hence does not show CP.

served in the CP amplitude spectrum around 2.09 eV [see Fig. 4(d)]. The (6,5) tubes embedded in P3HT, however, highlight the modulation and behave like local antenna for the nonstationary state in the polymer.

The optical band gap of PFO is higher in energy than that of P3HT; however the wrapping-induced planarization causes a sizable redshift of the optical band gap, bringing it down to about 2.5 eV [see inset of Fig. 2(b)] so that it is in resonance with the 7 fs visible broadband pulses. In Fig. 5(b), we show pump and probe spectra in PFO:CNT 500 fs after the pump pulse. Sharp bleaching features at 2.16 and 1.89 eV are assigned to the (6,5) and (7,5) tubes, respectively. Under these conditions, the CNTs are resonantly excited as well. CNT bleaching features however appear superposed to a broad PA band. PA in a similar spectral region is also seen in pure CoMoCat samples,[19] however with relative strength far below that of the respective bleach features. Figure 5(b) shows that in our case it is the opposite: the PA band overwhelms the bleach band. Consequently, we attribute the PA band to charged states in PFO.[28] Analogously to the case of P3HT:CNT, charge states can be intrinsic of the PFO network or caused by CNT-polymer charge transfer.

Time traces at fixed probe energies show strong coherent oscillations. In Fig. 5(a) (left inset) we show an FT map in the region around 1600 cm^{-1}. Over the whole range of probe energies, the FT peaks at frequencies around 1605 nm. Only near the maximum of the E_{22} resonance of the (6,5) tube we find an additional weak shoulder at 1590 cm^{-1}. We assign the 1605 cm^{-1} mode to the C=C double bond stretching of the polymer and the 1590 cm^{-1} vibration to the G mode of the (6,5) tube. [As an example, the FT spectrum taken at 2.16 eV displays the strong band at 1605 cm^{-1}, the shoulder at 1590 cm^{-1}, and a weaker peak at 310 cm^{-1} which is consistent with the radial breathing mode of the (6,5) tube.] In Fig. 5(c), we show the amplitude and phase profile for the PFO phonon at 1605 cm^{-1}. There is a minimum, together with a phase jump at 2.14 eV. This feature cannot be assigned to PFO, so again we find that the *polymer* coherent phonon spectrum shows an electronic transition of the CNT network. Here however there is an additional puzzle: the minimum is near but clearly downshifted in energy with respect to the E_{22} resonance for the (6,5) tube. The energetic position of the phase flip, exactly on top of the amplitude minimum, confirms however that what we see is the center frequency of the oscillating peak. Our speculation here is that we observe a modulation of the E_{22} exciton transition energy for a charged tube, in accordance with data obtained for chemically doped tubes.[29] The facts that the phase jump is slightly less than π and that the amplitude minimum does not reach zero but remains finite and can both be explained by disorder. Minor features around 1.95 eV can be to other tube types that undergo a similar mechanism when wrapped into the PFO polymer.

In conclusion, we reported transient CNT exciton resonance modulation in polymer-CNT composite for two quite different systems. We propose this be due to the transient modulation of the polymer matrix dielectric function induced by the coherent phonon (Raman effect). We assume that the exciton in the CNT follows adiabatically this modulation, resulting in a nonstationary screening of the *e-h* interaction. A few observations can be made: (i) the one dimensional character of the CNT exciton leads to a large "sampling" of the Coulomb field onto the surrounding tube volume, thus demonstrating the importance of the embedding medium; (ii) the phonon energy is about 0.2 eV, compared to the exciton binding energy of about 0.5 eV and an exciton transition energy for E_{22} of 2.5 eV. This places our system into the intermediate dielectric coupling regime. Therefore, the adiabatic following has to be checked in detail by a specific calculation and cannot be simply approximated. The experimental facts rest however as an indication that this is indeed the case.

This work reports an example of stationary and transient dielectric screening in polymer-CNT composite which certainly highlights the great sensitivity of CNT to the environment. In our tentative model, we push forward our speculation to a conjecture on the atomic structure: The polymer C=C stretch frequency is so strongly affecting the E_{22} reso-

nance energy of the CNT because it affects the bond-length alternation which in turn acts upon the *commensurateness* of the polymer-carbon positions with the ideal hexagonal CNT "surface," with significant affects on the CNT exciton stabilization. This model is to be proved by quantum-chemical calculations on a variety of levels, which is the focus of a forthcoming study.

This work was financially supported by the European Commission through the Human Potential Programme (Marie-Curie RTN BIMORE, Grant No. MRTN-CT-2006-035859). We thank Tobias Hertel and Jared Crochet for the absorption spectrum of the polymer-free CoMoCat samples in Fig. 2(a).

*Corresponding author. FAX: +34 914976855; larry.luer@imdea.org

[1] P. Avouris, Y. H. Chen, and V. Perebeinos, Nat. Nanotechnol. **2**, 605 (2007).
[2] V. Perebeinos, J. Tersoff, and P. Avouris, Phys. Rev. Lett. **92**, 257402 (2004).
[3] V. Perebeinos and P. Avouris, Nano Lett. **7**, 609 (2007).
[4] M. Kanungo, H. Lu, G. G. Maillaras, and G. B. Blanchet, Science **323**, 234 (2009).
[5] B. R. Goldsmith, J. G. Coroneus, V. R. Khalap, A. A. Kane, G. A. Weiss, and P. G. Collins, Science **315**, 77 (2007).
[6] A. Nish, J.-Y. Hwang, J. Doig, and R. J. Nicholas, Nat. Nanotechnol. **2**, 640 (2007).
[7] M. Giulianini, E. R. Waclawik, J. M. Bell, M. Scarselli, P. Castrucci, M. De Crescenzi, and N. Motta, Appl. Phys. Lett. **95**, 143116 (2009).
[8] D. A. Yarotski, S. V. Kilina, A. A. Talin, S. Tretiak, O. V. Prezhdo, A. V. Balatsky, and A. J. Taylor, Nano Lett. **9**, 12 (2009).
[9] A. Nish, J.-Y. Hwang, J. Doig, and R. J. Nicholas, Nanotechnology **19**, 095603 (2008).
[10] G. D. Sanders, C. J. Stanton, J. H. Kim, K. J. Yee, Y. S. Lim, E. H. Hároz, L. G. Booshehri, J. Kono, and R. Saito, Phys. Rev. B **79**, 205434 (2009).
[11] A. Gambetta, C. Manzoni, E. Menna, M. Meneghetti, G. Cerullo, G. Lanzani, S. Tretiak, A. Piryatinski, A. Saxena, R. L. Martin, and A. R. Bishop, Nat. Phys. **2**, 515 (2006).
[12] J.-H. Kim, J. Park, B. Y. Lee, D. Lee, K. J. Yee, Y. S. Lim, L. G. Booshehri, E. H. Hároz, J. Kono, and S. H. Baik, J. Appl. Phys. **105**, 103506 (2009).
[13] K. Kato, K. Ishioka, M. Kitajima, J. Tang, R. Saito, and H. Petek, Nano Lett. **8**, 3102 (2008).
[14] F. Chen, B. Wang, Y. Chen, and L.-J. Li, Nano Lett. **7**, 3013 (2007).
[15] D. Polli, L. Luer, and G. Cerullo, Rev. Sci. Instrum. **78**, 103108 (2007).
[16] H.-J. Egelhaaf, D. Oelkrug, W. Gebauer, M. Sokolowski, E. Umbach, T. Fischer, and P. Baeuerle, Opt. Mater. **9**, 59 (1998). The molar extinction coefficient per thiophene ring is reported as $\varepsilon_{Thiophene} \approx 8000\ M^{-1}\ cm^{-1}$ yielding a natural (base e) absorption cross section of $\sigma_{Thiophene} \approx 3 \times 10^{-17}\ cm^2$. Assuming that only the four carbon atoms per thiophene ring contribute to the absorption, we obtain the reported value.
[17] M. Zheng and B. Diner, J. Am. Chem. Soc. **126**, 15490 (2004).
[18] J. Clark, C. Silva, R. H. Friend, and F. C. Spano, Phys. Rev. Lett. **98**, 206406 (2007).
[19] Z. Zhu, J. Crochet, M. S. Arnold, M. S. Hersam, H. Ulbricht, D. Resasco, and T. Hertel, J. Phys. Chem. C **111**, 3831 (2007).
[20] S. M. Bachilo, M. S. Strano, C. Kittrell, R. H. Hauge, R. E. Smalley, and R. B. Weisman, Science **298**, 2361 (2002).
[21] L. Lüer, S. Hoseinkhani, D. Polli, J. Crochet, T. Hertel, and G. Lanzani, Nat. Phys. **5**, 54 (2009).
[22] I. Gurevitch and S. Srebnik, Chem. Phys. Lett. **444**, 96 (2007).
[23] L. Lüer, C. Gadermaier, J. Crochet, T. Hertel, D. Brida, and G. Lanzani, Phys. Rev. Lett. **102**, 127401 (2009).
[24] G. Lanzani, in *Coherent Vibrational Spectroscopy*, Practical Spectroscopy Series Vol. 36, edited by S. De Silvestri, G. Cerullo, and G. Lanzani (CRC Press/Taylor & Francis, Boca Raton, FL, 2008).
[25] G. Lanzani, M. Zavelani-Rossi, G. Cerullo, D. Comoretto, and G. Dellepiane, Phys. Rev. B **69**, 134302 (2004).
[26] O. J. Korovyanko, R. Österbacka, X. M. Jiang, and Z. V. Vardeny, Phys. Rev. B **64**, 235122 (2001).
[27] G. Louarn, M. Trznadel, J. P. Buisson, J. Laska, A. Pron, M. Lapovski, and S. Lefrant, J. Phys. Chem. **100**, 12532 (1996).
[28] T. Virgili, G. Cerullo, L. Luer, G. Lanzani, C. Gadermaier, and D. D. C. Bradley, Phys. Rev. Lett. **90**, 247402 (2003).
[29] K. K. Kim, J. J. Bae, H. K. Park, S. M. Kim, H.-Z. Geng, K. A. Park, H.-J. Shin, S. M. Yoon, A. Benayad, J.-Y. Choi, and Y. H. Lee, J. Am. Chem. Soc. **130**, 12757 (2008).